The Cartilage-Bone Interface

Caroline D. Hoemann, Ph.D.[1,2,3] Charles-Hubert Lafantaisie-Favreau, M.Sc.[2]
Viorica Lascau-Coman, M.Sc.[1,3] Gaoping Chen, M.D.[1] Jessica Guzmán-Morales, Ph.D.[1]

[1] Department of Chemical Engineering, Ecole Polytechnique, Montreal, Quebec, Canada
[2] Institute of Biomedical Engineering, Ecole Polytechnique, Montreal, Quebec, Canada
[3] Groupe de Recherche en Sciences et Technologies Biomédicales (GRSTB), Ecole Polytechnique, Montreal, Quebec, Canada

Address for correspondence and reprint requests Caroline D. Hoemann, Ph.D., Department of Chemical Engineering, Ecole Polytechnique, 2900 Boulevard Edouard-Montpetit, Montreal, Quebec H3G 1J4, Canada (e-mail: caroline.hoemann@polymtl.ca).

J Knee Surg

Abstract

In the knee joint, the purpose of the cartilage-bone interface is to maintain structural integrity of the osteochondral unit during walking, kneeling, pivoting, and jumping–during which tensile, compressive, and shear forces are transmitted from the viscoelastic articular cartilage layer to the much stiffer mineralized end of the long bone. Mature articular cartilage is integrated with subchondral bone through a ~20 to ~250 μm thick layer of calcified cartilage. Inside the calcified cartilage layer, perpendicular chondrocyte-derived collagen type II fibers become structurally cemented to collagen type I osteoid deposited by osteoblasts. The mature mineralization front is delineated by a thin ~5 μm undulating tidemark structure that forms at the base of articular cartilage. Growth plate cartilage is anchored to epiphyseal bone, sometimes via a thin layer of calcified cartilage and tidemark, while the hypertrophic edge does not form a tidemark and undergoes continual vascular invasion and endochondral ossification (EO) until skeletal maturity upon which the growth plates are fully resorbed and replaced by bone. In this review, the formation of the cartilage-bone interface during skeletal development and cartilage repair, and its structure and composition are presented. Animal models and human anatomical studies show that the tidemark is a dynamic structure that forms within a purely collagen type II-positive and collagen type I-negative hyaline cartilage matrix. Cartilage repair strategies that elicit fibrocartilage, a mixture of collagen type I and type II, are predicted to show little tidemark/calcified cartilage regeneration and to develop a less stable repair tissue-bone interface. The tidemark can be regenerated through a bone marrow-driven growth process of EO near the articular surface.

Keywords
- endochondral ossification
- tidemark
- calcified cartilage
- articular cartilage
- collagen type II
- collagen type I
- bone
- blood vessels
- growth plate
- glycosaminoglycan

All Cartilage-Bone Interfaces Are Derived from an Initially Pure Cartilage Structure

Long bones develop first from embryonic mesenchymal stem cells that coalesce to form a "blastema," with a scant but uniform type I collagen matrix.[1] The blastema transforms at early fetal stages into a cartilaginous structure, or cartilage "anlage," with collagen type II as the main extracellular component.[2–6] The cartilage "anlage" contains a mixture of fusiform and round chondroblast cells,[7] that upon terminal differentiation will hypertrophy (become unusually large), and begin to express proteins that attract blood vessels and facilitate biomineralization.[8]

Mineralized bone begins to form when the fetal cartilage undergoes focal hypertrophy which launches a process of endochondral ossification (EO). The very first cartilage-bone interfaces to form in the body are at the primary ossification centers in the shaft of developing long bones. These areas are

received
November 21, 2011
accepted after revision
March 26, 2012

DOI http://dx.doi.org/10.1055/s-0032-1319782.
ISSN 1538-8506.

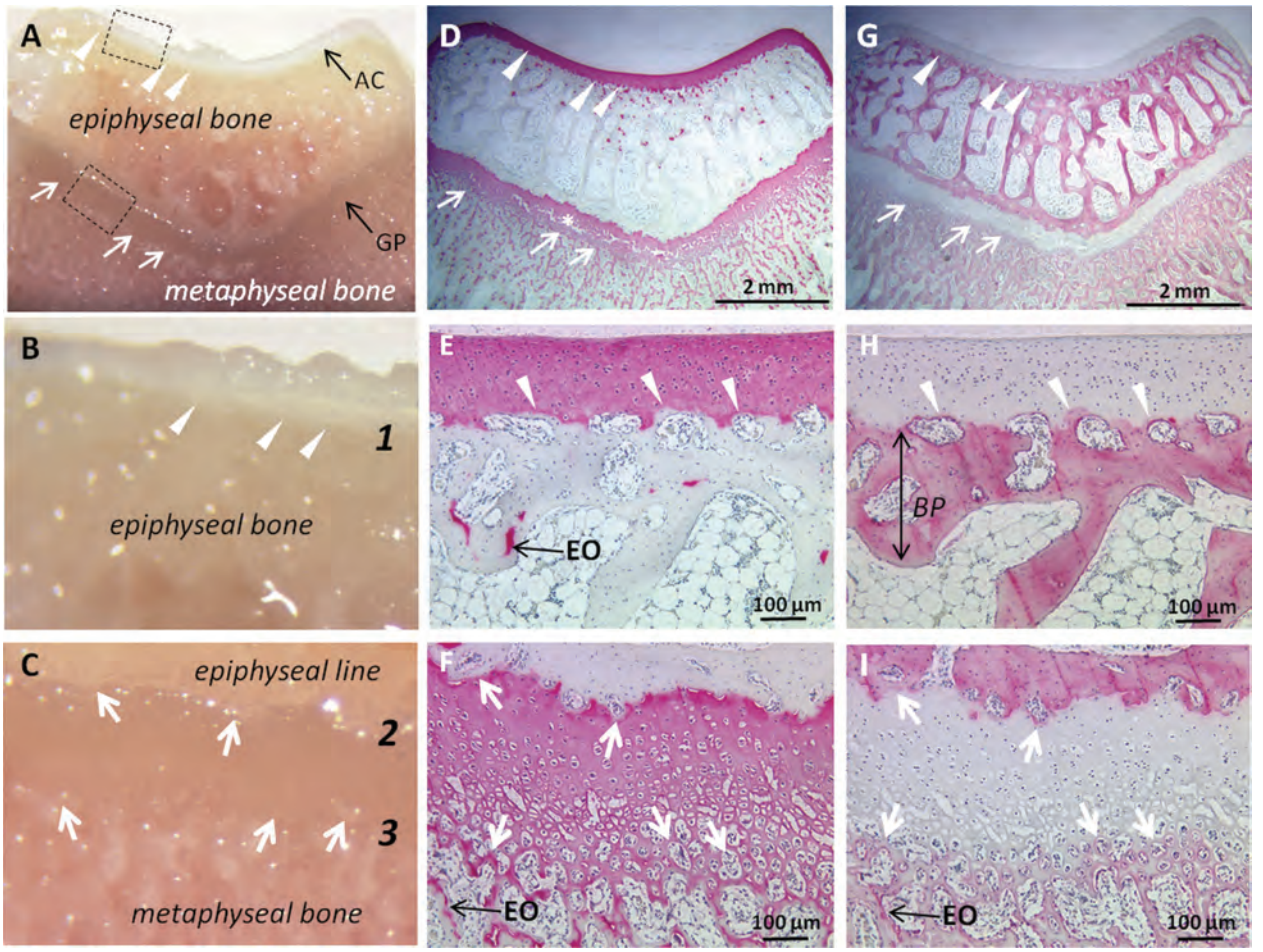

Figure 1 Three dynamic cartilage-bone interfaces are established in the postnatal knee femoral end: (1) articular cartilage-epiphyseal bone, (2) growth plate-epiphyseal bone, and (3) growth plate-metaphyseal bone. A macroscopic transverse view of a skeletally immature ~4-month rabbit knee trochlea shows the articular cartilage (AC, white arrowheads, A & B) and growth plate (GP, white arrows, A & C), and distribution of collagen type II (D, E, F) and collagen type I (G, H, I) in serial sections from the area of the dashed squares in panel A. The distal femur was fixed in 4% paraformaldehyde/100 mM cacodylate, decalcified in EDTA with a Milestone microwave, cryoembedded and cryosectioned using the CryoJane tape system; the sections were predigested in hyaluronidase and protease to remove glycosaminoglycans and immunostained for collagen type II (monoclonal II6B3, DSHB, USA) or collagen type I (monoclonal antibody I-H85, VWR, Canada), using secondary biotinylated goat antimouse and avidin-alkaline phosphatase red substrate detection with iron hematoxylin counterstain.[91,92] In panels A and B, the rough articular surface is a cutting artifact from the isomet diamond saw. The tear/crack in the growth plate indicated by a white asterisk in panel D is a cryosectioning artifact.[92] EO, endochondral ossification; BP, subchondral bone plate; AC, articular cartilage; GP, growth plate.

marked by remodeling and vascular invasion in parallel with the deposition of a mineralizing collagen type I matrix that ensheathes and mechanically protects the blood vessels.[4,9] After the secondary ossification centers appear in the distal tibia and femur, three types of dynamic cartilage-bone interface are established, as illustrated in the immature rabbit knee (►**Fig. 1A–C**). Articular cartilage sits on top of the epiphyseal subchondral bone (►**Fig. 1B, E, H**). The growth plate is a cartilage structure firmly sandwiched between two layers of bone: the epiphyseal and the metaphyseal bone (►**Fig. 1C, F, I**).

Growth Plate Cartilage-Bone Interfaces during Postnatal Development

In the developing knee, epiphyseal bone will continue to expand into the cartilage anlage until the cartilage interface forms a thin calcified layer that arrests vascular invasion. Calcified cartilage forms at the base of the articular cartilage, and in certain growth plate reserve zones (►**Fig. 2**), through mechanisms that are still not fully understood. Haines[10] previously noticed that growth plate reserve zones fused to "permanent" epiphyseal lines develop a thin layer of calcified cartilage/tidemark (►**Fig. 2A**, proximal trochlea) while other reserve zones do not form tidemarks (►**Fig. 2B**, distal trochlea) and eventually close without leaving a scar.

Growth plate hypertrophic cartilage (HTC) does not form a tidemark. This interface is actually a mixture of cartilage and bone, by definition of the primary spongiosa, where new bone is deposited on the cartilage trabeculae carved out by invading blood vessels and marrow (►**Figs. 1F, I,** and **3**). In trabecular bone maturing below the growth plate, an initially pure collagen type II-glycosaminoglycan (GAG) extracellular matrix is slowly incorporating collagen type I (EO, ►**Fig. 3**). Vascular invasion of

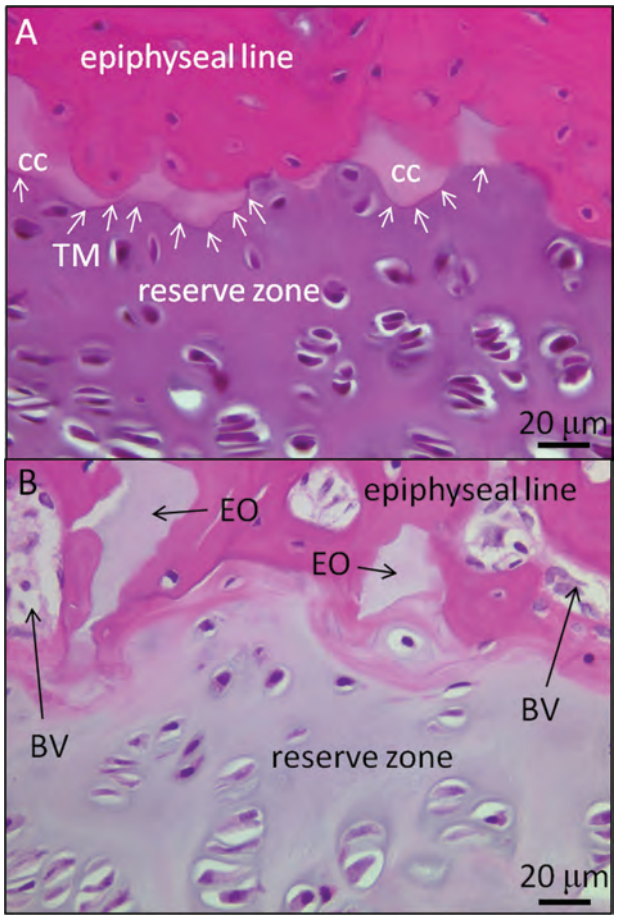

Figure 2 The growth plate-epiphyseal bone interface sometimes includes a layer of calcified cartilage and a tidemark in the reserve zone (A, proximal trochlea), and in other areas is devoid of calcified cartilage or tidemark and fused to a more vascular bone (B, distal trochlea). Representative decalcified transverse sections from ~4-month-old rabbit trochlear growth plates stained with hematoxylin and eosin are shown, from $N = 7$ distinct New Zealand white rabbit femurs, ~4 months old. TM, tidemark (white arrows); BV, blood vessels; CC, calcified cartilage; EO, endochondral ossification (cartilage remnant).

the hypertrophic zone spurs a continual endochondral expansion of the distal femur (arrows, ►**Fig. 4A**), in tandem with appositional cartilage and bone growth (►**Fig. 4B, C**).

The growth cartilage-metaphyseal bone interface is a dynamic and ever-expanding front of HTC undergoing vascular invasion and ossification. Interestingly, in newly formed endochondral bone, hypertrophic chondrocytes express zymogen forms of enzymes capable of remodeling collagen matrix, including matrix metalloproteinases (MMP-13, MMP-9) and complement C1s.[11,12] In knockout mice for MMP-13 or MMP-9, conversion of collagen type II HTC to collagen type I trabecular bone is inhibited.[13–15] Remodeling of the HTC front by osteoclasts, chondroclasts, and bone-marrow-derived metalloproteinases drives the replacement of HTC with vascularized bone.[13–15] Growth plate cell proliferation and vascular invasion can be diminished by nutritional deprivation, ischemia, or supraphysiologic loading.[16–18] Blood vessel invasion of the HTC layer is believed to be naturally driven by hypertrophic chondrocyte secretion of angiogenic factors,[19] MMP-13,[11,13] and gelatinases capable of untethering matrix-bound vascular endothelial growth factor.[15] Osteoclasts that remodel the base of endochondral bone are also known to release angiogenic factors and can also promote vascular invasion and osteogenesis.[20,21] Apoptosis of hypertrophic chondrocytes is also implicated as an important driver of the endochondral growth process.[15,22]

Articular Cartilage-Bone Interface during Postnatal Development

A distinct and more advanced EO process is going on during postnatal articular cartilage growth (►**Fig. 1E** and **H**). In 3- to 6-month-old rabbit articular cartilage, most chondrocytes are no longer proliferating, and a tidemark has formed at the base of the hypertrophic zone.[23] Bone is not being deposited along cartilage trabeculae, it has developed layer-by-layer to form a thick osteoid around blood vessels subjacent to the calcified cartilage layer. Only small patches of cartilage persist in the subchondral bone (EO, ►**Fig. 1E**). The remnants of GAG and collagen type II in trabecular bone are the hallmarks of EO.

Neonatal articular cartilage is relatively thick; it is filled with a system of endothelial-lined canals distinct from the normal vasculature.[7] Cartilage canals have been described in immature articular cartilage in a variety of large animals and in human (fetal ovine, 2-week-old calf, 2-year-old human).[7,24] Postnatal weight-bearing activity is associated with regression of the canals, and a thinning and anisotropic organization of the articular cartilage layer. The articular layer continues to grow postnatally through an appositional or asymmetric layer-by-layer expansion, through cell division near the superficial zone[6,25,26] (►**Fig. 4**). In the deep zone near the articular cartilage-bone interface, chondrocytes terminally differentiate into hypertrophic chondrocytes, cease to proliferate, and express collagen type II, collagen type X, alkaline phosphatase, and osteopontin, a highly phosphorylated hydroxylapatite-binding protein.[27–31] Like articular cartilage, the growth plate hypertrophic zone also contains collagen type X and alkaline phosphatase, but a tidemark is notably absent.[32,33] The tidemark that forms at the base of mature articular cartilage develops slightly below the region of chondrocytes expressing collagen type X.[28] Mineral deposits form in the neonatal calcified layer of the articular cartilage in line with the collagen fibers.[34] Using fluorescent pulse labeling of the mineral phase, Oegema et al observed that the tidemark advances above the pulse-labeled mineralization front in 4-month-old rabbit patella at a rate of 8 µm/week, compared with 1 µm/week in the 7-month-old rabbit patella.[26] Creeping advancement of the tidemark is associated with thinning of the articular cartilage layer.[23]

Vascular channels are branched structures that supply the calcified cartilage of the articular layer,[7,9,35] and have similarities with vascular channels in the vertebral endplate where bone abuts the cartilaginous nucleus pulposus.[36] The calcified cartilage zone is thus normally vascularized, while the non-mineralized cartilage above the tidemark is normally avascular. In a study by Bonde et al,[37] blood vessels were observed to

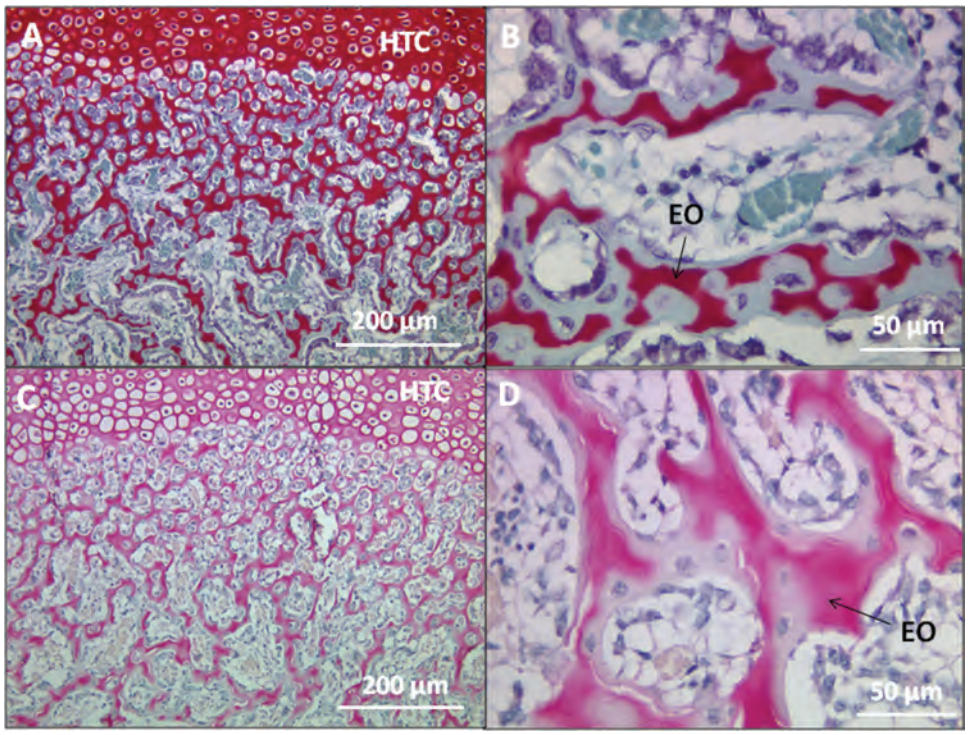

Figure 3 Newly synthesized endochondral metaphyseal bone below the growth plate of a 4-month-old rabbit contains abundant sulfated glycosaminoglycans (GAG, red Safranin O stain, panels A, B) and collagen type II (pink immunostain, panels C, D) in addition to collagen type I (in this figure, the collagen type I matrix has been counterstained green by fast green in A, B, or blue by hematoxylin in C, D). In panel B, fast green counterstain also shows bone marrow and blood vessels. A 4-month-old rabbit knee femur end was fixed in formalin, decalcified in 0.5N HCl/0.1% glutaraldehyde, cut transversely in the trochlea, embedded in paraffin, and stained with Safranin O/Fast green/Iron hematoxylin or immunostained for collagen type II as previously described.[60,72,91] Examples of cartilage remnant present in the primary spongiosa formed by EO are indicated in B and D. EO, endochondral ossification; HTC, hypertrophic cartilage.

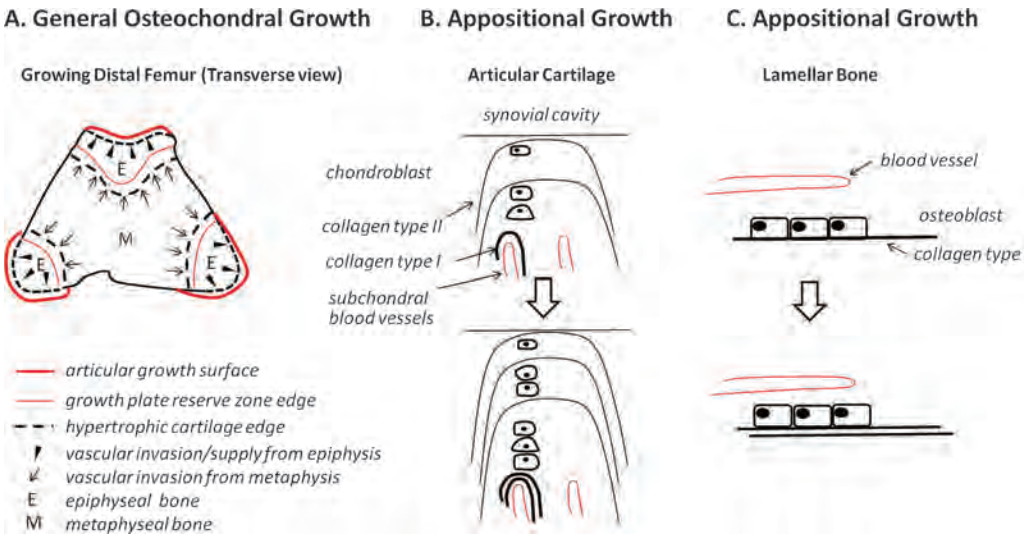

Figure 4 Illustration of femur growth and appositional growth. (A) The distal femur grows (as illustrated in faithful tracings of a transverse section through the immature rabbit trochlea and proximal condyles) through vascular invasion which drives endochondral ossification of the hypertrophic zone of the growth plates (arrows, thick dashed lines) while blood vessels from the epiphyseal bone supply the articular cartilage hypertrophic zone (arrowheads). During appositional growth of articular cartilage (B), proliferating chondroblasts deposit fibrillar collagen type II above a previously existing layer of collagen type II; the proliferating chondrocytes are situated above invading blood vessels frequently capped with collagen type I-positive mineralized bone. In intramembranous bone growth (C), osteoblasts and blood vessels are closely associated during inframembranous generation of lamellar bone. The mechanisms of endochondral bone growth are not illustrated in this diagram.

Table 1 Published Histomorphometric and Stereological Measures of Articular Cartilage, Tidemark, Calcified Cartilage, Bone Plate Thickness, and Tidemark Number or Area Normal and OA Human Subjects, and Different Animal Species

	N/OA	Age	Site	Articular Cartilage (μm)	Tidemark (Number or Area)	Calcified Cartilage (μm)	Bone Plate
Lane and Bullough 1980[44]	NH	20–39	FH	—	1.2 ± 0.1	193 ± 28	—
Lane and Bullough 1980[44]	NH	40–59	FH	—	1.2 ± 0.1	141 ± 18	—
Lane and Bullough 1980[44]	NH	60–93	FH	—	1.8 ± 0.4	119 ± 24	—
Frisbie et al 2006 [48]	NH	—	MFC	2200	—	125	490
Frisbie et al 2006[48]	NE	—	MFC	2000	—	210	375
Frisbie et al 2006[48]	NO	—	MFC	450	—	125	250
Frisbie et al 2006[48]	NR	—	MFC	200	—	100	250
Hunziker et al 2002[46]	NH	23–49	MFC	2410	—	134	190
Wang et al 2009[43]	NH	20–45	MFC[a]	—	—	104 ± 21	—
Bonde et al 2005[37]	NH	65–85	PAT	—	2.5 cm^2 (1.8–3.9)[b]	—	—
Bonde et al 2005[37]	OA	47–86	MFC	—	7.7 cm^2 (2.4–13.3)[c]	—	—

[a]Weight-bearing area.
[b]Mean 0.5 (0 to 10) penetrating blood vessels in non-OA patellar tidemark.
[c]Mean 9 penetrating blood vessels (2 to 47) in OA tidemark area, 3 out of 21 vessels had thrombosis.
—, not done; FH, femoral head; MFC, medial femoral condyle; NH, normal human; OA, OA human; NE, normal equine; NO, normal ovine; NR, normal rabbit, PAT, patella.

only sporadically penetrate the tidemark into cartilage in normal patellar cadaveric subjects (less than 1 average blood vessel per normal patella from subjects 75 to 89 years old) compared with an average of nine tidemark-penetrating vessels per subject in osteoarthritis (OA) femoral condyle samples. Pathologic blood vessel passage beyond the tidemark is associated with occasional thrombosis, a thicker calcified cartilage layer, and tidemark duplication[37] (►**Table 1**).

The calcified cartilage layer is semipermeable and permits passage of small molecules (<500 Da) from the subchondral bone to the articular cartilage layer.[38,39] Conversely, immersion of a mouse distal femur end in fluorescein allows full solute passage through the articular cartilage and selective fluorescein diffusion into chondrocytes in the calcified cartilage layer.[39] Calcified cartilage permeability was measured as fivefold less than noncalcified cartilage in mature horse metacarpal tissues.[38] It has been hypothesized that venous congestion in the synovium and subchondral bone could play a role in tidemark duplication.[37] Thickening of the calcified cartilage in OA could be expected to reduce the flow of small solutes from the vascularized subchondral bone to the deep zone chondrocytes.

Once formed, the tidemark and calcified cartilage layer persist as dynamic structures that can change and remodel over time. Below mature articular cartilage, the mineralization front is a relatively smooth and undulating plate-like surface, as illustrated in a micro-computed tomography (micro-CT) 3-D image of the calcified cartilage and bone below the trochlear articular cartilage in a 30-month-old rabbit knee (►**Fig. 5A**). The tidemark at this stage is a strong hematoxylin-stained line (►**Fig. 5B**). Some remnant or newly duplicating tidemarks can be observed within the mature calcified cartilage layer (open arrowheads, ►**Fig. 5B**). In the skeletally immature 4-month-old rabbit, a more irregular mineralization front is observed at the articular cartilage-bone interface, which corresponds to the subchondral bone and a thin layer of calcified cartilage (►**Fig. 5C**). At this stage a nascent tidemark can be visualized using a hematoxylin & eosin stain, and the vascular bone channels are just below, with close communication between the vasculature and calcified articular cartilage (►**Fig. 5D**). By contrast, in the same 4-month-old rabbit trochlear specimen, the growth plate HTC contains a highly irregular and discontinuous mineralization front at the growing bone-cartilage interface with no visible tidemark (►**Fig. 5E, F**). The mineral front at the base of the growth plate corresponds with the vascular bone and newly deposited collagen type I (black arrowheads, ►**Fig. 5F**). In the growth plate hypertrophic zone, calcification of the collagen type II matrix is much delayed compared with the articular cartilage calcified layer. This is because after birth, the mammalian joints require a suitable mechanically stable articular surface, while growth plates in the long bones are continually expanding, even beyond sexual maturity. Cartilage calcification is therefore only occurring at the end-stage of cartilage growth. After reaching skeletal maturity, growth plates are completely resorbed and replaced by collagen type I–positive mineralized bone.

To summarize, growth plates develop a relatively stable reserve zone-epiphyseal bone interface, with a purely collagen type II GAG-rich cartilage phase, and a mixture of collagen type I and collagen type II in the newly forming primary spongiosa. Calcified cartilage becomes established at the edges of a "permanent" epiphyseal bone layer (i.e., proximal reserve zone and articular cartilage hypertrophic zone), and the tidemark serves as a barrier to vascular invasion and calcification of hyaline cartilage.

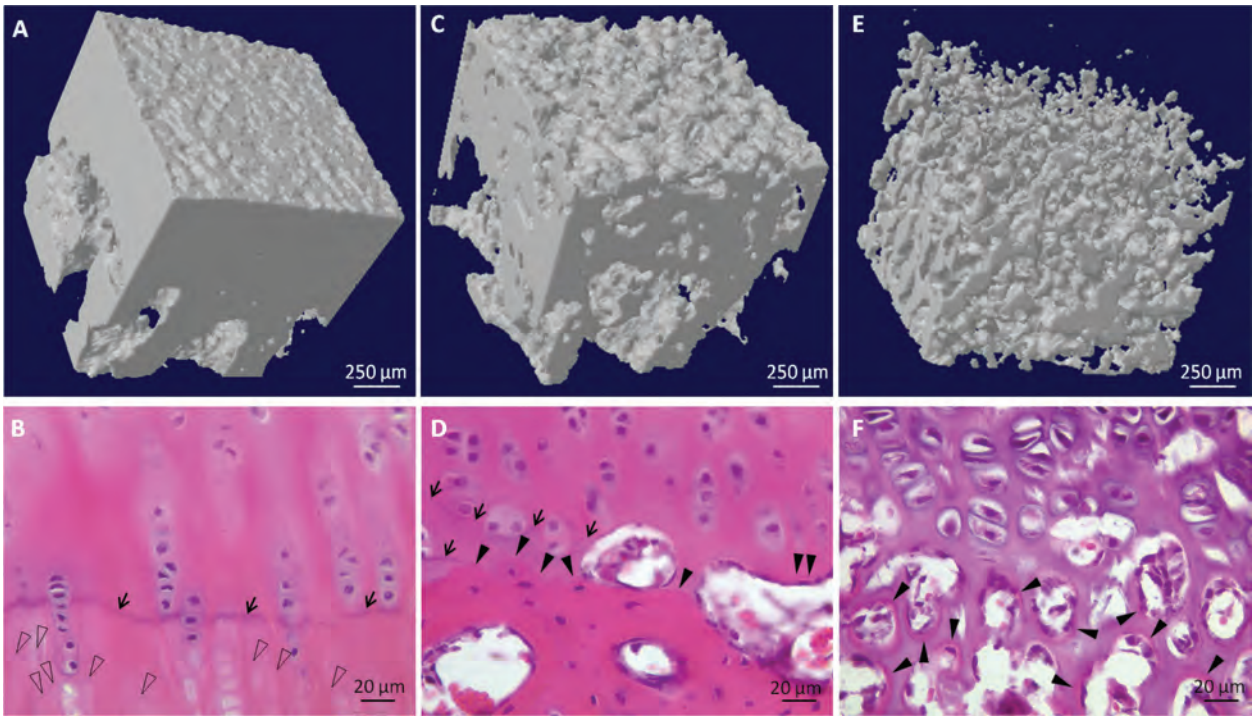

Figure 5 The mineralization front at the cartilage-bone interface, in a skeletally aged 30-month-old rabbit trochlea articular cartilage-subchondral bone plate (A, B), and skeletally immature 4-month-old rabbit articular cartilage-epiphyseal bone interface (C, D) and hypertrophic growth plate-metaphyseal bone interface (E, F). Panels A, C, and E show 3D reconstructions from a microcomputed tomography scan (SkyScan 1172 instrument, 9.8 µm/pixel resolution, NRecon and CTAn software) from the 30-month-old rabbit (A), and the 4-month-old rabbit trochlea shown in ►**Fig. 1C, E**. Panels B, D, and F show the histological appearance of the cartilage-bone interface from the 30-month-old (B), and 4-month-old rabbit trochlea (D, F), Hematoxylin & eosin stain. The small black arrows show the tidemark. Open arrowheads show vestigial or newly duplicating tidemarks (B) and the solid black arrowheads show areas of bone osteoid.

Structure and Mineral Content of the Mature Articular Cartilage-Bone Interface

Articular calcified cartilage is a mineralized layer where extracellular matrix is chiefly composed of collagen type II, collagen type X, and GAG[19]; the layer also contains extracellular alkaline phosphatase.[31] Alkaline phosphatase can generate free phosphate from organophosphates such as β-glycerol phosphate, for incorporation into hydroxylapatite mineral (Ca-P).[40–42] In the calcified cartilage layer of normal human femoral condyles, chondrocytes are quiescent and present at a much lower density compared with hyaline cartilage (average of 51 cells/mm^2 *versus* 152 cells/mm^2).[43] The calcified cartilage layer is flanked by an undulating tidemark, and an even more irregular cement line adjacent to the bone. Wang et al[43] analyzed normal adult human bone (20- to 45-year-old cadaveric) by histomorphometry and stereology to show that hyaline cartilage is interlocked tightly in a "ravine-engomphosis" structure with the calcified cartilage zone, which is then attached in a "comb-anchor" to bone.[43] The surface roughness was determined to be 1.14 (tidemark) and 1.99 (cement line).[43] The more irregular cement line-bone interface is the end result of an inhomogeneous vascular invasion during development of the calcified cartilage layer (white arrowheads, ►**Fig. 1H**).

In normal human subjects, the mean calcified cartilage thickness is variable, from 20 µm to ~250 µm.[44–46] The calcified cartilage is tightly fused to the articular cartilage and subchondral bone plate composed of lamellar bone, along with punctate regions where the calcified cartilage is in direct contact with vascular channels.[7,47] In any group of individuals, the mean calcified cartilage thickness and mineral density will vary according to age, site in the joint, and mechanical loading (►**Table 1**).[44,48,49] In a study of normal femoral head cadaveric specimens with no signs of OA by Lane and Bullough,[44] the calcified cartilage thickness in the femoral head varied from 79 µm to 243 µm, with a thicker calcified cartilage in less stressed areas of the hip joint. Muller-Gerbl et al[45] performed a similar study in normal cadaveric femur heads, and found the calcified cartilage thickness varied from 20 µm to 230 µm, and that the ratio of calcified cartilage to total cartilage thickness was relatively constant. The calcified cartilage layer shows gradual thinning with age, along with tidemark duplication in subjects over 70 years old (see ►**Table 1**).[44] Lane and Bullough concluded that the calcified layer is undergoing continual resorption and endochondral advancement over time.[44] These observations are consistent with the measured dwindling rate of advancement of the tidemark with age in rabbit patella.[26] In 31 normal human femoral condyles, an age-dependent loss in bone mass was measured in the subchondral bone plate.[50] The bone volume fraction (Bone Volume/Total Volume%) of the bone plate region was observed to decline from ~36% for subjects in their 20's to ~27% for those >80 years old.[50] Bone loss was

attributed to thinning of the subchondral trabeculae with age (as opposed to diminished trabecular number), and this occurred at a relatively steady rate (Trabecular Thickness = 141 μm-0.63 × age).[50] By contrast, in OA, a pathological increase in the calcified cartilage layer thickness arises, along with abnormal tidemark duplication[37] (see Bonde, ►**Table 1**), and this is frequently accompanied by subchondral bone plate thickening and sclerosis.[51] The consequence or implication of tidemark duplication is not known, although Burr has proposed that microcracks at the bone-cartilage interface may be implicated in the etiology.[51]

The mineral component in the calcified cartilage layer is similar but distinct from that found in bone, and notably influenced by the uniform presence of GAG. In a study by Rey et al, pulverized calcifying cartilage from 2-month-old calves (collagen type II-positive and type I-negative) had a very low mineral content (2.8% by weight), with an immature, very poorly crystalline and low carbonate apatite mineral [calcium/(phosphate + carbonate)], compared with bone (normally ~0.20 carbonate/P).[41] The calcified cartilage mineral phase was also characterized by a large proportion of nonapatite "brushite-like" phosphate.[41] Unlike bone, this high nonmineral, labile phosphate content actually increases over time.[41] The low mineral content measured in immature calcified cartilage by Rey et al[41] is consistent with the quite irregular mineral surface of the epiphyseal growth plate shown in ►**Fig. 5C**. In this sample, the mineral surface most probably corresponds to mineralized collagen type I, as the threshold level used in this 3-dimensional reconstruction model would remove hypomineralized calcified cartilage from the image (i.e., areas between the black arrows and black arrowheads, ►**Fig. 5D**).

In situ elemental analyses of the skeletally mature normal human or OA human cartilage-bone interface has revealed the presence of calcium, phosphorus, potassium, sulfur, zinc, and strontium.[52,53] In mature osteochondral samples, the mineralized surface has a smoother texture and corresponds to the tidemark, with no visible difference by micro-CT between the calcified cartilage and osteoid immediately below (►**Fig. 5A, B**).[54] In a normal human patella, mineralized cartilage showed a slightly but significantly higher calcium content than adjacent bone (25% vs. 23% w/v), and the mineral particles in bone and articular calcified cartilage were found to align with the direction of collagen organization.[55] Using 2-dimensional nuclear magnetic resonance (2D-NMR) spectroscopy and X-ray diffraction, Duer et al[56] analyzed the mineral component of pulverized calcified cartilage samples from skeletally mature horse phalanx and distal radius. They concluded that the calcified cartilage mineral signal is similar to hydroxyapatite of bone, but with smaller peaks indicating small crystals or disorder in the mineral component. They also found evidence that unlike bone, GAG present in calcified cartilage provides a more hydrated matrix, and provides anionic side-chains (carboxylate and sulfate) for binding calcium in the mineral crystal surfaces, and the hydroxyl groups to H-bond with surface water, mineral hydroxyl, and phosphate ions.[56] The spectra were also consistent with the presence of Gla residues (γ-carboxy glutamic acid) in the calcified cartilage layer; Gla-domain proteins are found in a variety of mineral-binding proteins such as osteocalcin.[27]

It is not well understood how the tidemark is formed, and knowledge of its precise composition is also limited. The tidemark is a 5 μm thick structure that appears at the cartilage-calcified cartilage junction and can be visualized with hematoxylin, a blue dye that is intensified by metal ions. The tidemark could potentially arise simply by the accumulation and precipitation of chondrocyte-derived extracellular matrix species and ions at the calcified cartilage front, due to the sharp decrease in tissue permeability. The tidemark could serve to inhibit calcifying matrix vesicles released from the bone from penetrating into hyaline cartilage. Lectin staining has suggested that the tidemark contains variously branched alkali-resistant glycans with β-galactosyl or N-acetyl-lactosamine termini.[57] Zoeger et al[53] detected a specific accumulation of lead at the tidemark in normal cadaveric femoral head and patella. Oegema et al suggested that the superficial articular layer could be involved in a paracrine loop that controls deep zone chondrocyte hypertrophy and calcification, which could potentially explain thickening of the calcified cartilage in OA following loss of the superficial zone.[26] Alternatively, microcracks in the calcified layer could permit diffusion of bone-derived matrix vesicles farther into the deep zone, resulting in tidemark advancement.

Duplication of the tidemark in aging and OA is well documented.[26,44,51,58] In aging subjects, up to 5 duplicated tidemarks were observed in normal human subjects over 70 years old,[44] and as many as 10 tidemarks in primates over 20 years old.[58] A significant correlation was observed between increasing tidemark duplication, mineral density, and carbonate content in primates.[58] Repetitive knee microtrauma in a rabbit model during 9 weeks of loading was shown to lead to a mean 25% increase in the proximal tibial calcified cartilage layer thickness, and tidemark duplication, with no change in mean articular cartilage thickness.[59] Multiple tidemarks were observed to form at the cartilage-bone interface in tissues surrounding an osteochondral defect in rabbit trochlea 6 months postoperative,[60] and in sheep above a metal implant placed in the subchondral bone.[59] Tidemark duplication could be related to uneven load-sharing following softening of a focal area of damaged cartilage.[60]

Cartilage-Bone Interface in Cartilage Repair

In articular cartilage lesions, the tidemark is either fully retained (Outerbridge grade I to III partial-thickness lesions), or missing to a variable extent (grade IV full-thickness lesions).[61] Most cartilage repair procedures start with debridement of the surface of the lesion to remove degenerated articular cartilage.[62] Depending on the repair approach, the debridement step may aim to retain the calcified cartilage layer for cell delivery[63–65] or to completely remove it, as during microfracture or marrow stimulation.[66–68] However if present, the tidemark and calcified cartilage are technically very challenging to debride with precision. Light curettage usually leaves a thin layer of noncalcified deep zone articular

cartilage, while shaving or vigorous curettage often removes a considerable amount of subchondral bone plate with the calcified cartilage.[54,64,65] Vascular channels containing erythrocytes terminate normally inside the calcified cartilage layer.[7] Therefore, in a joint with only one tidemark, debridement of the tidemark along with as little as 50 µm of the superficial mineralized layer is expected to generate some bleeding at the debrided surface, although bleeding from these tiny capillaries may not be macroscopically visible. Skeletally immature animals have a greater ease of debridement and different cell populations present in the epiphysis compared with the adult knee (►**Figs. 1** and **5**). In addition, the epiphyseal blood vasculature in skeletally immature knees has active endothelial cell proliferation while adult vasculature has postmitotic endothelia and the subchondral bone no longer contains osteoclasts.[21] It is for these reasons that skeletally immature animals are improper cartilage repair models for adult knees.[69] These same cautionary notes hold for rats and mice, whose growth plates never close.

Scarce information is available on tidemark regeneration. One may reasonably wonder whether tidemark regeneration should be one of the goals of cartilage repair strategies. Frisbie et al showed that tidemark could regenerate in equine microfractured defects at 12 months postoperative only if the calcified cartilage layer were completely debrided.[70] In lesions that retained calcified cartilage and original tidemark, the new repair tissue had poor tissue integration with the base of the defect.[70] Sheep femoral condyle microfracture defects treated or not with a chitosan-based implant showed partial tidemark regeneration at 6 months postoperative, at the base of hyaline-like cartilage (HyC) repair with a collagen type II-positive and collagen type I-negative deep zone fully integrated with bone.[71,72] In an equine case study, a cartilage defect treated by deep debridement and a composite implant regenerated a tidemark at 12 months postoperative in repair cartilage with a deep zone containing appropriate collagen fiber organization.[73] In a rabbit microdrill model of cartilage repair, a tidemark was observed at 6 months postoperative where the bone and cartilage tissue formed an integrated unit.[60]

Several groups have shown that chondrogenic foci will spontaneously form in drill or microfracture holes generated in skeletally mature knee cartilage defects.[74–77] Subchondral cartilage repair tissue contains cells with chondrocyte morphology that normally progress to hypertrophy, vascular invasion, and replacement by bone.[21,60,74–78] Chevrier et al[75] concluded that chondrogenic foci that appear near the top of the drill holes can mature to acquire a stratified structure with vascular invasion and endochondral resorption at the base after 2 months in a rabbit model, leaving an articular layer of hyaline repair cartilage.

In various models of marrow stimulation in the rabbit, microdrill holes that are created and left to bleed (as in clinical practice[79]) will spontaneously regenerate a fibrocartilage repair tissue that contains both collagen type I and collagen type II.[21,60,78] This type of spontaneous repair in a rabbit is illustrated in ►**Fig. 6**, at 2.5 months postoperative. In this rabbit, using a small arthrotomy, a 1.4 mm diameter, 2 mm deep microdrill hole was created in the distal femoral knee trochlea and allowed to bleed without further treatment. After 2.5 months postoperative, the drilled defect is still undergoing EO and repair. The drill hole has spontaneously regenerated fibrocartilage repair at the top of the drill hole, which is anchored to HTC that sits below the tidemark within the flanking articular cartilage (►**Fig. 6A–C**). Endochondral vascular invasion and mineralization are occurring at base of the HTC (black arrowheads, ►**Fig. 6A–E**). Patches of GAG and collagen type II in the new repair bone trabeculae reveal the "tell-tale signs" of EO (►**Fig. 6A–D**). From the histology drawing shown in ►**Fig. 6D**, we can appreciate that EO has been initiated at a previous time point in this defect, because the patches of GAG which reveal remnants of hyaline cartilage in the newly formed bone occur in areas up to 400 µm below the blunted mineralization front (►**Fig. 6D–F**). The morphology of the endochondral repair tissue at this point, including cryosectioning tears, resembles that of the growth plate and no tidemark is visible.

In the same animal described above, a 1.4 mm diameter, 2 mm deep microdrill hole was created in the left knee trochlea and further treated by press-fitting a presolidified chitosan-blood implant into the hole.[80] Relative to the contralateral untreated drill hole, after 2.5 months of repair, a delayed and altered EO process is seen in the treated defect (►**Fig. 7**). HyC repair tissue containing low levels of collagen type II and no collagen type I is observed above the mineralization front (►**Fig. 7B, C**). The hyaline-like repair is overlaid with undifferentiated mesenchyme surrounded by collagen type I (►**Fig. 7C**). In this implant-treated defect, the mineralization front has a more irregular appearance and consists in bony vascular invasion of hyaline tissue (►**Fig. 7F**). One can appreciate that in this osteochondral defect, the implant has delayed osteochondral ossification because the mineralized GAG is only beginning to form at the repair cartilage-bone interface (EO, ►**Fig. 7A, D, E**). Unlike the endochondral bone formed during spontaneous repair, hypertrophic chondrocytes are scarcely present at the advancing interface of new bone and blood vessels (►**Fig. 8**). Collagen type I of newly formed bone is being deposited from inside the invading bone marrow channels. Given that the chondrocytes present in the collagen type II repair matrix are not yet terminally differentiated to hypertrophic cells, the proximity of repair cells and invading blood vasculature can still drive cell proliferation and appositional growth of more collagen type II hyaline-like matrix. At one edge of the drill hole, the bone has regenerated to the native tidemark level, and a new tidemark can be observed (►**Fig. 9**).

In some rabbit cartilage repair models involving complete debridement of the calcified cartilage layer, subchondral bone plate advancement beyond the native tidemark in flanking cartilage has been observed after 3 to 9 months of repair.[81,82] Bone plate advancement could be a consequence of delayed or failed tidemark regeneration during bone marrow-driven EO below hyaline-like repair tissue.

In human cartilage repair, the extent of tidemark formation in repair osteochondral biopsies has been added to a new histological scoring system generated by the International

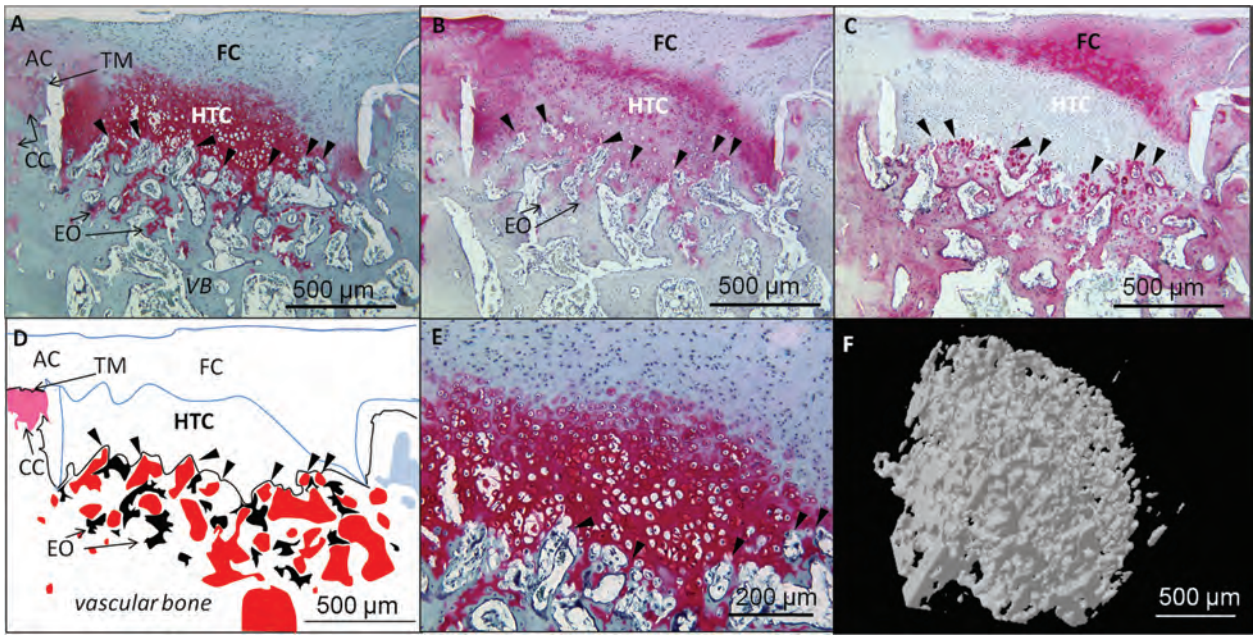

Figure 6 Spontaneous repair of a 1.4 mm diameter, 2 mm deep osteochondral drill hole at 2.5 months postoperative in the knee trochlea of a skeletally aged (32 months) rabbit. Decalcified serial cryosections through the drill hole were stained for SafraninO/Fast green (A, E), or immunostained for collagen type II (B) or type I (C). The articular cartilage repair tissue is characterized as fibrocartilage or fibrous because it contains mainly collagen type I with little collagen type II and is depleted of GAG. Panel D shows faithful tracings of structures from Panel A, including bone-associated GAG as a marker of endochondral ossification (EO, black), angiogenic bone marrow cavities (red), hypertrophic cartilage (HTC), and fibrocartilage (FC). Mineral formation below hypertrophic cartilage during endochondral ossification is shown in Panel F, by a reconstructed 3-D image from a micro-CT scan (SkyScan 1172, 9.8 µm/pixel resolution, area corresponding to panel E) that was performed prior to decalcification. All protocols involving animals were approved by Institutional Ethics Committees. Symbols: AC, articular cartilage; FC, fibrocartilage; TM, tidemark; CC, calcified cartilage; EO, endochondral ossification; HTC, hypertrophic cartilage area; VB, vascular bone; arrowheads, bone mineralization front.

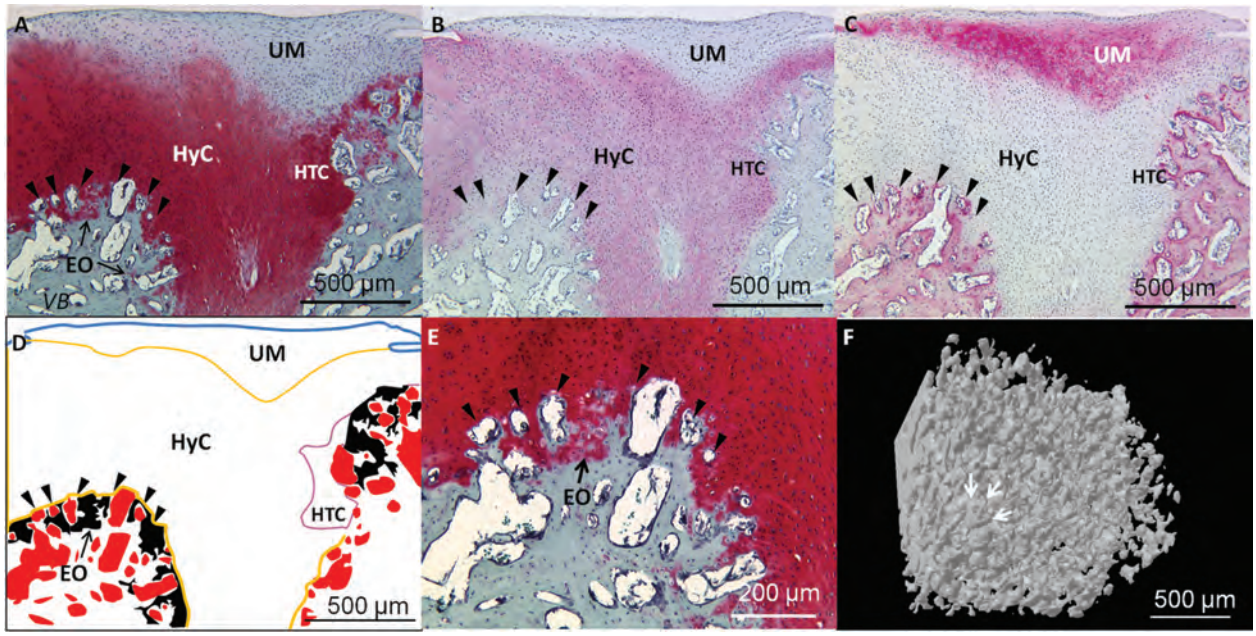

Figure 7 Repair of a 1.4 mm diameter, 2 mm deep osteochondral drill hole at 2.5 months postsurgery in the knee trochlea of a skeletally mature (32 months) rabbit, where the drill hole was treated at surgery by press-fitting a presolidified chitosan-NaCl/autologous whole blood clot implant into the hole.[80] The defect was generated in the contralateral knee of the rabbit defect shown in ►**Fig. 6**, under institutionally approved animal protocols. At 2.5 months postoperative, femur ends were fixed, micro-CT scanned (Skyscan 1172, 9.8 µm/pixel resolution), decalcified in EDTA, and cryosections stained for Safranin O/Fast green (panels A, E), immunostained for collagen type II (B), or collagen type I (C). Panel D shows tracings of structures in Panel A, including bone-associated GAG as a marker of EO (black), angiogenic marrow cavities (red), HyC, area of HTC, and UM. Panel F shows a reconstructed 3D image from a micro-CT scan corresponding to the area shown in (E). Black arrowheads: mineralization front. The three white arrows in panel F show a bone-encased blood vessel very similar to a branched vascular invasion histology image previously published by Oegema.[26] HyC, hyaline-like cartilage; HTC, hypertrophic cartilage area; EO, endochondral ossification; UM, undifferentiated mesenchyme; arrowheads, mineralization front.

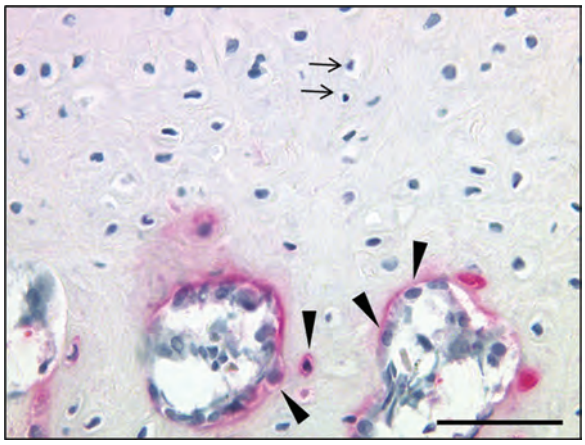

Figure 8 Developing cartilage-bone interface in the subchondral area of an osteochondral defect treated with a presolidified chitosan-based implant at 2.5 months postoperative (from the same histology image shown in ►**Fig. 7C**). The section was immunostained for collagen type I (red stain) with iron hematoxylin counterstain. Arrows show round and crescent-shaped chondrocyte cells in hyaline-like repair cartilage and arrowheads show collagen type I-expressing cells that cap the invading blood vessel bone marrow cavities with new osteoid, similar to that described by Gilmore and Palfrey in neonatal human lateral femoral articular cartilage.[7] Both round and cuboidal cells express collagen type I, as is seen in growth plate endochondral bone. Scale bar: 50 µm.

Cartilage Repair Society (ICRS II).[83] The score uses a visual analog scale (VAS) where the reader marks a line on a 10 mm scale that is then converted to a percentage between 0% (no tidemark) to 100%. In one randomized controlled clinical trial comparing characterized chondrocyte implantation (CCI) and microfracture (MFX), osteochondral repair biopsies were analyzed in a blinded fashion using the ICRS II scoring system. At 12 months postoperative, both CCI and MFX groups showed the same ~16-point mean clinical improvement from baseline in overall KOOS score[84] that progressed to ~20 CCI versus ~15 MFX mean change from baseline KOOS at 5 years postoperative ($p = 0.116$).[85] Biopsies collected at 12 months postoperative from 48 out of 61 MFX-treated patients showed a mean ~18% tidemark formation along the biopsy width compared with a mean ~32% tidemark formation in biopsies from 38 out of 51 CCI-allocated patients ($p = 0.036$).[84] Given that cell therapy aims to retain the calcified cartilage layer at surgery,[86] significantly greater tidemark present in CCI biopsies could be partly due to a lighter debridement of the initial tidemark in the CCI lesions.

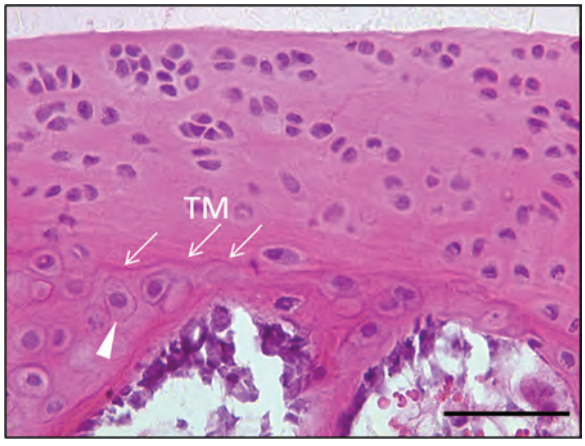

Figure 9 Evidence of tidemark formation at 2.5 months postoperative at the edge of the repairing rabbit trochlear osteochondral hole at the level of the tidemark, in an osteochondral drill hole treated with presolidified chitosan-blood implant. Hematoxylin-eosin stained EDTA-decalcified cryosection. The arrows show the new tidemark (TM) and the arrowhead shows a terminally differentiated hypertrophic chondrocyte inside the newly forming calcified cartilage layer. The image was taken from a field near the upper right corner of ►**Fig. 7A**. Scale bar: 50 µm.

Another randomized controlled clinical trial compared MFX to MFX and chitosan-glycerol phosphate/blood implant (BST-CarGel), at 12 months postoperative.[87,88] Blinded ICRS II scoring of osteochondral biopsies revealed more tidemark present in nine biopsies from MFX-treated defects compared with 12 implant-treated defects.[88] Some biopsies from this study showed zonal collagen organization resembling native articular cartilage,[89] and a hyaline-like deep zone containing collagen type II and no collagen type I.[87,88] One MFX biopsy collected at 12 months postoperative consisted in a collagen type I + /collagen type II+ fibrocartilage repair with an irregular bone interface, and 0% tidemark formation.[72]

To summarize, tidemark has been observed in some human cartilage repair osteochondral biopsies 12 months following bone marrow stimulation or cell therapy. The presence of a tidemark could arise through hyaline cartilage regeneration via EO, or by incomplete debridement and persistence of the native tidemark in the treated lesion. Finally, despite great care, it is also possible that some biopsies with a complete tidemark may have been taken from outside the area of the initial lesion.[72]

Cartilage repair is a complex process that takes place over a long period of time. The notion of cartilage repair as an isolated event should be discarded for the more comprehensive view of osteochondral repair, given the extensive cross-talk between cartilage repair tissues, bone, and blood vessels in the developing interface. New calcified cartilage layer/tidemark can be regenerated in a pure type II collagen matrix containing GAG integrated to endochondral bone near the articular surface. Residual cartilage and calcified cartilage can block cell migration and vascular invasion during marrow-derived cartilage regeneration, therefore, new tools or methods that permit the surgeon to verify the presence of residual cartilage and calcified cartilage at the debridement step would help control this important variable. To better evaluate the progression and success of different cartilage repair therapies, patient-reported outcomes[90] need to be correlated with repair tissue architecture.[72] A better understanding of cartilage repair tissue maturity will be reached with new histological methods that can distinguish between native and regenerated tidemark, standardized measures of tidemark and calcified cartilage formation, and further research on the mechanisms of cartilage calcification.

Summary Points and Clinical Relevance

1. All cartilage-bone interfaces develop from an initially cartilaginous structure that undergoes coordinated invasion by blood vessels and osteoblasts. Formation of a tidemark anatomically stabilizes the cartilage-bone interface and arrests cartilage calcification and blood vessel invasion. Vascularization of the calcified cartilage layer and subchondral bone plate is an important feature of a healthy cartilage-bone interface.
2. The cartilage-bone interface is a mineralized blood vessel boundary where collagen type II is integrated with collagen type I.
3. Animals that have permanently open growth plates (mice and rats), and skeletally immature animals with open growth plates (rabbits less than 7-months old, and large animals less than ~2 years old), are improper cartilage repair models for establishing the efficacy of therapies intended for use in adult human knees.
4. Chronic medications (i.e., steroids), drugs (i.e., smoking), or surgical procedures that produce chronic ischemia in the epiphyseal bone may contribute to articular cartilage degeneration and/or suppress cartilage regeneration. Conversely, treatments that stimulate revascularization of subchondral bone damaged by drilling or microfracture have the potential to drive epiphyseal endochondral repair.
5. With increasing age, microtrauma, and advanced OA, the calcified cartilage layer either thins out, or thickens and becomes more mineralized (►**Fig. 5A vs. 5C**, ►**Table 1**). Therefore, when carrying out clinical surgical procedures that aim to debride the calcified cartilage layer, the potential thickness and extent of mineralization of the calcified cartilage layer should be taken into account.
6. Calcified cartilage and osteoid in the adult subchondral bone have a similar mineral level, which means that during debridement procedures, the tidemark can only be fully removed by cleanly and carefully scraping off a specific mineralized depth from the entire lesional surface.
7. The tidemark and calcified cartilage layer are technically very challenging to debride with precision. Light curettage usually leaves a thin layer of noncalcified deep zone articular cartilage, while shaving or vigorous curettage often removes a considerable amount of subchondral bone plate with the calcified cartilage. In a joint with only one tidemark, debridement of the tidemark along with as little as 50 μm of the superficial mineralized layer is expected to generate bleeding, that may or may not be immediately visible.
8. Bone plate advancement could be a consequence of delayed or failed tidemark regeneration during bone marrow-driven EO below hyaline-like repair tissue.
9. When evaluating outcomes of cartilage repair procedures, it is important to realize that the presence of a tidemark could arise through true hyaline cartilage regeneration or by incomplete debridement and persistence of the native tidemark.

Acknowledgments

Funding for this work was from the Canadian Institutes of Health Research (CIHR, 185810-BME), Natural Sciences and Engineering Research Council of Canada (NSERC, STGP 365025), the Canada Foundation for Innovation (CFI), and Fonds de Recherche Santé du Québec (FRSQ, Groupe de Recherche en Sciences et Technologies Biomédicales, GRSTB). Salary support for C.D.H. was from an FRSQ bourse Chercheur National/National Researcher Career Award. We thank Geneviève Picard and Jun Sun for excellent technical contributions, and Julie Tremblay for Quality Assurance.

References

1 Sasano Y, Mizoguchi I, Kagayama M, Shum L, Bringas P Jr, Slavkin HC. Distribution of type I collagen, type II collagen and PNA binding glycoconjugates during chondrogenesis of three distinct embryonic cartilages. Anat Embryol (Berl) 1992;186(3):205–213
2 Craig FM, Bentley G, Archer CW. The spatial and temporal pattern of collagens I and II and keratan sulphate in the developing chick metatarsophalangeal joint. Development 1987;99(3):383–391
3 Olsen BR, Reginato AM, Wang W. Bone development. Annu Rev Cell Dev Biol 2000;16(10810706):191–220
4 Sandberg M, Vuorio E. Localization of types I, II, and III collagen mRNAs in developing human skeletal tissues by in situ hybridization. J Cell Biol 1987;104(4):1077–1084
5 Shapiro F. Bone development and its relation to fracture repair. The role of mesenchymal osteoblasts and surface osteoblasts. Eur Cell Mater 2008;15:53–76
6 Hunziker EB. The elusive path to cartilage regeneration. Adv Mater (Deerfield Beach Fla) 2009;21(32-33):3419–3424
7 Gilmore RS, Palfrey AJ. A histological study of human femoral condylar articular cartilage. J Anat 1987;155:77–85
8 Leboy PS, Vaias L, Uschmann B, Golub E, Adams SL, Pacifici M. Ascorbic acid induces alkaline phosphatase, type X collagen, and calcium deposition in cultured chick chondrocytes. J Biol Chem 1989;264(29):17281–17286
9 Clark JM. The structure of vascular channels in the subchondral plate. J Anat 1990;171:105–115
10 Haines RW. The histology of epiphyseal union in mammals. J Anat 1975;120(Pt 1):1–25
11 D'Angelo M, Yan Z, Nooreyazdan M, et al. MMP-13 is induced during chondrocyte hypertrophy. J Cell Biochem 2000;77(4): 678–693
12 Sakiyama H, Inaba N, Toyoguchi T, et al. Immunolocalization of complement C1s and matrix metalloproteinase 9 (92kDa gelatinase/type IV collagenase) in the primary ossification center of the human femur. Cell Tissue Res 1994;277(2):239–245
13 Stickens D, Behonick DJ, Ortega N, et al. Altered endochondral bone development in matrix metalloproteinase 13-deficient mice. Development 2004;131(23):5883–5895
14 Little CB, Meeker CT, Hembry RM, et al. Matrix metalloproteinases are not essential for aggrecan turnover during normal skeletal growth and development. Mol Cell Biol 2005;25(8):3388–3399
15 Vu TH, Shipley JM, Bergers G, et al. MMP-9/gelatinase B is a key regulator of growth plate angiogenesis and apoptosis of hypertrophic chondrocytes. Cell 1998;93(3):411–422
16 Reich A, Jaffe N, Tong A, et al. Weight loading young chicks inhibits bone elongation and promotes growth plate ossification and vascularization. J Appl Physiol 2005;98(6):2381–2389
17 Farnum CE, Lee AO, O'Hara K, Wilsman NJ. Effect of short-term fasting on bone elongation rates: an analysis of catch-up growth in young male rats. Pediatr Res 2003;53(1):33–41

18 Kim HK, Su P-H, Qiu Y-S. Histopathologic changes in growth-plate cartilage following ischemic necrosis of the capital femoral epiphysis. An experimental investigation in immature pigs. J Bone Joint Surg Am 2001;83-A(5):688–697

19 Alini M, Matsui Y, Dodge GR, Poole AR. The extracellular matrix of cartilage in the growth plate before and during calcification: changes in composition and degradation of type II collagen. Calcif Tissue Int 1992;50(4):327–335

20 Cackowski FC, Anderson JL, Patrene KD, et al. Osteoclasts are important for bone angiogenesis. Blood 2010;115(1):140–149

21 Chen G, Sun J, Lascau-Coman V, Chevrier A, Marchand C, Hoemann CD. Acute osteoclast activity following subchondral drilling is promoted by chitosan and associated with improved cartilage tissue integration. Cartilage 2011;2:173–185

22 Hashimoto S, Ochs RL, Rosen F, et al. Chondrocyte-derived apoptotic bodies and calcification of articular cartilage. Proc Natl Acad Sci U S A 1998;95(6):3094–3099

23 Hunziker EB, Kapfinger E, Geiss J. The structural architecture of adult mammalian articular cartilage evolves by a synchronized process of tissue resorption and neoformation during postnatal development. Osteoarthritis Cartilage 2007;15(4):403–413

24 Namba RS, Meuli M, Sullivan KM, Le AX, Adzick NS. Spontaneous repair of superficial defects in articular cartilage in a fetal lamb model. J Bone Joint Surg Am 1998;80(1):4–10

25 Hayes AJ, MacPherson S, Morrison H, Dowthwaite G, Archer CW. The development of articular cartilage: evidence for an appositional growth mechanism. Anat Embryol (Berl) 2001;203(6): 469–479

26 Oegema TR Jr, Carpenter RJ, Hofmeister F, Thompson RC Jr. The interaction of the zone of calcified cartilage and subchondral bone in osteoarthritis. Microsc Res Tech 1997;37(4):324–332

27 Heinegård D, Oldberg A. Structure and biology of cartilage and bone matrix noncollagenous macromolecules. FASEB J 1989; 3(9):2042–2051

28 Gannon JM, Walker G, Fischer M, Carpenter R, Thompson RC Jr, Oegema TR Jr. Localization of type X collagen in canine growth plate and adult canine articular cartilage. J Orthop Res 1991;9(4): 485–494

29 Jiang J, Leong NL, Mung JC, Hidaka C, Lu HH. Interaction between zonal populations of articular chondrocytes suppresses chondrocyte mineralization and this process is mediated by PTHrP. Osteoarthritis Cartilage 2008;16(1):70–82

30 Sundaramurthy S, Mao JJ. Modulation of endochondral development of the distal femoral condyle by mechanical loading. J Orthop Res 2006;24(2):229–241

31 Stephens M, Kwan APL, Bayliss MT, Archer CW. Human articular surface chondrocytes initiate alkaline phosphatase and type X collagen synthesis in suspension culture. J Cell Sci 1992;103(Pt 4): 1111–1116

32 Ali SY, Sajdera SW, Anderson HC. Isolation and characterization of calcifying matrix vesicles from epiphyseal cartilage. Proc Natl Acad Sci U S A 1970;67(3):1513–1520

33 Shum L, Nuckolls G. The life cycle of chondrocytes in the developing skeleton. Arthritis Res 2002;4(2):94–106

34 Robinson RA, Cameron DA. Electron microscopy of the primary spongiosa of the metaphysis at the distal end of the femur in the newborn infant. J Bone Joint Surg Am 1958;40-A(3): 687–697

35 Boyde A, Firth EC. Articular calcified cartilage canals in the third metacarpal bone of 2-year-old thoroughbred racehorses. J Anat 2004;205(6):491–500

36 Kobayashi S, Baba H, Takeno K, et al. Fine structure of cartilage canal and vascular buds in the rabbit vertebral endplate. Laboratory investigation. J Neurosurg Spine 2008;9(1): 96–103

37 Bonde HV, Talman MLM, Kofoed H. The area of the tidemark in osteoarthritis—a three-dimensional stereological study in 21 patients. APMIS 2005;113(5):349–352

38 Arkill KP, Winlove CP. Solute transport in the deep and calcified zones of articular cartilage. Osteoarthritis Cartilage 2008;16(6): 708–714

39 Pan J, Zhou XZ, Li W, Novotny JE, Doty SB, Wang LY. In situ measurement of transport between subchondral bone and articular cartilage. J Orthop Res 2009;27(10):1347–1352

40 Bellows CG, Aubin JE, Heersche JNM. Initiation and progression of mineralization of bone nodules formed in vitro: the role of alkaline phosphatase and organic phosphate. Bone Miner 1991;14(1): 27–40

41 Rey C, Beshah K, Griffin R, Glimcher MJ. Structural studies of the mineral phase of calcifying cartilage. J Bone Miner Res 1991;6 (5):515–525

42 Hoemann CD, El-Gabalawy H, McKee MD. In vitro osteogenesis assays: influence of the primary cell source on alkaline phosphatase activity and mineralization. Pathol Biol (Paris) 2009;57(4): 318–323

43 Wang FY, Ying Z, Duan XJ, et al. Histomorphometric analysis of adult articular calcified cartilage zone. J Struct Biol 2009;168(3): 359–365

44 Lane LB, Bullough PG. Age-related changes in the thickness of the calcified zone and the number of tidemarks in adult human articular cartilage. J Bone Joint Surg Br 1980;62(3):372–375

45 Müller-Gerbl M, Schulte E, Putz R. The thickness of the calcified layer of articular cartilage: a function of the load supported? J Anat 1987;154:103–111

46 Hunziker EB, Quinn TM, Häuselmann HJ. Quantitative structural organization of normal adult human articular cartilage. Osteoarthritis Cartilage 2002;10(7):564–572

47 Lyons TJ, McClure SF, Stoddart RW, McClure J. The normal human chondro-osseous junctional region: evidence for contact of uncalcified cartilage with subchondral bone and marrow spaces. BMC Musculoskelet Disord 2006;7:52

48 Frisbie DD, Cross MW, McIlwraith CW. A comparative study of articular cartilage thickness in the stifle of animal species used in human pre-clinical studies compared to articular cartilage thickness in the human knee. Vet Comp Orthop Traumatol 2006;19(3): 142–146

49 Madry H, van Dijk CN, Mueller-Gerbl M. The basic science of the subchondral bone. Knee Surg Sports Traumatol Arthrosc 2010; 18(4):419–433

50 Koszyca B, Fazzalari NL, Vernon-Roberts B. Calcified cartilage, subchondral and cancellous bone morphometry within the knee of normal subjects. Knee 1996;3:15–22

51 Burr DB, Schaffler MB. The involvement of subchondral mineralized tissues in osteoarthrosis: quantitative microscopic evidence. Microsc Res Tech 1997;37(4):343–357

52 Kaabar W, Iaklouk A, Bunk O, Baily M, Farquharson MJ, Bradley D. Compositional and structural studies of the bone-cartilage interface using PIXE and SAXS techniques. Nuclear Instruments & Methods in Physics Research Section Accelerators Spectrometers Detectors and Associated Equipment 2010;619(1–3):78–82

53 Zoeger N, Roschger P, Hofstaetter JG, et al. Lead accumulation in tidemark of articular cartilage. Osteoarthritis Cartilage 2006; 14(9):906–913

54 Marchand C, Chen HM, Buschmann MD, Hoemann CD. Standardized three-dimensional volumes of interest with adapted surfaces for more precise subchondral bone analyses by micro-computed tomography. Tissue Eng Part C Methods 2011;17(4):475–484

55 Zizak I, Roschger P, Paris O, et al. Characteristics of mineral particles in the human bone/cartilage interface. J Struct Biol 2003;141(3):208–217

56 Duer MJ, Friscić T, Murray RC, Reid DG, Wise ER. The mineral phase of calcified cartilage: its molecular structure and interface with the organic matrix. Biophys J 2009;96(8):3372–3378

57 Lyons TJ, Stoddart RW, McClure SF, McClure J. The tidemark of the chondro-osseous junction of the normal human knee joint. J Mol Histol 2005;36(3):207–215

58 Miller LM, Novatt JT, Hamerman D, Carlson CS. Alterations in mineral composition observed in osteoarthritic joints of cynomolgus monkeys. Bone 2004;35(2):498–506
59 Burr DB. Anatomy and physiology of the mineralized tissues: role in the pathogenesis of osteoarthrosis. Osteoarthritis Cartilage 2004;12(Suppl A):S20–S30
60 Marchand C, Chen G, Tran-Khanh N, et al. Microdrilled cartilage defects treated with thrombin-solidified chitosan/blood implant regenerate a more hyaline, stable, and structurally integrated osteochondral unit compared to drilled controls. Tissue Eng Part A 2012;18(5–6):508–519
61 Cameron ML, Briggs KK, Steadman JR. Reproducibility and reliability of the outerbridge classification for grading chondral lesions of the knee arthroscopically. Am J Sports Med 2003;31(1):83–86
62 Mithoefer K, McAdams TR, Scopp JM, Mandelbaum BR. Emerging options for treatment of articular cartilage injury in the athlete. Clin Sports Med 2009;28(1):25–40
63 Peterson L, Minas T, Brittberg M, Nilsson A, Sjögren-Jansson E, Lindahl A, Sjögren-Jansson E. Two- to 9-year outcome after autologous chondrocyte transplantation of the knee. Clin Orthop Relat Res 2000;374(374):212–234
64 Drobnic M, Radosavljevic D, Cör A, Brittberg M, Strazar K. Debridement of cartilage lesions before autologous chondrocyte implantation by open or transarthroscopic techniques: a comparative study using post-mortem materials. J Bone Joint Surg Br 2010;92(4):602–608
65 Mika J, Clanton TO, Pretzel D, Schneider G, Ambrose CG, Kinne RW. Surgical preparation for articular cartilage regeneration without penetration of the subchondral bone plate: in vitro and in vivo studies in humans and sheep. Am J Sports Med 2011;39(3):624–631
66 Steadman JR, Rodkey WG, Singleton SB, Briggs KK. Microfracture technique for full-thickness chondral defects: technique and clinical results. Oper Tech Orthop 1997;7(4):300–304
67 Mithoefer K, Williams RJ III, Warren RF, et al. The microfracture technique for the treatment of articular cartilage lesions in the knee. A prospective cohort study. J Bone Joint Surg Am 2005;87(9):1911–1920
68 Knutsen G, Engebretsen L, Ludvigsen TC, et al. Autologous chondrocyte implantation compared with microfracture in the knee. A randomized trial. J Bone Joint Surg Am 2004;86-A(3):455–464
69 Hurtig MB, Buschmann MD, Fortier LA, et al. Preclinical Studies for Cartilage Repair: Recommendations from the International Cartilage Repair Society. Cartilage. 2011;2(2):137–152
70 Frisbie DD, Morisset S, Ho CP, Rodkey WG, Steadman JR, McIlwraith CW. Effects of calcified cartilage on healing of chondral defects treated with microfracture in horses. Am J Sports Med 2006;34(11):1824–1831
71 Hoemann CD, Hurtig M, Rossomacha E, et al. Chitosan-glycerol phosphate/blood implants improve hyaline cartilage repair in ovine microfracture defects. J Bone Joint Surg Am 2005;87(12):2671–2686
72 Hoemann CD, Kandel R, Roberts S, et al. International Cartilage Repair Society (ICRS) Recommended Guidelines for Histological Endpoints for Cartilage Repair Studies in Animal Models and Clinical Trials. Cartilage 2011;2(2):153–172
73 Kon E, Mutini A, Arcangeli E, et al. Novel nanostructured scaffold for osteochondral regeneration: pilot study in horses. J Tissue Eng Regen Med 2010;4(4):300–308
74 Shapiro F, Koide S, Glimcher MJ. Cell origin and differentiation in the repair of full-thickness defects of articular cartilage. J Bone Joint Surg Am 1993;75(4):532–553
75 Chevrier A, Hoemann CD, Sun J, Buschmann MD. Temporal and spatial modulation of chondrogenic foci in subchondral microdrill holes by chitosan-glycerol phosphate/blood implants. Osteoarthritis Cartilage 2011;19(1):136–144
76 Hoemann CD, Chen G, Marchand C, et al. Scaffold-guided subchondral bone repair: implication of neutrophils and alternatively activated arginase-1+ macrophages. Am J Sports Med 2010;38(9):1845–1856
77 Chevrier A, Hoemann CD, Sun J, Buschmann MD. Chitosan-glycerol phosphate/blood implants increase cell recruitment, transient vascularization and subchondral bone remodeling in drilled cartilage defects. Osteoarthritis Cartilage 2007;15(3):316–327
78 Chen H, Hoemann CD, Sun J, et al. Depth of subchondral perforation influences the outcome of bone marrow stimulation cartilage repair. J Orthop Res 2011;29(8):1178–1184
79 Insall JN. Intra-articular surgery for degenerative arthritis of the knee. A report of the work of the late K. H. Pridie. J Bone Joint Surg Br 1967;49(2):211–228
80 Guzmàn-Morales J, Lafantaisie-Favreau C, Sun J, Rivard G, Hoemann CD. Analysis of the mid-term effects of chitosan-NaCl/blood pre-solidified implants in an in vivo osteochondral repair model. Paper presented at: International Cartilage Repair Society, 25 Sept, 2010; Barcelona, Spain.
81 Qiu YS, Shahgaldi BF, Revell WJ, Heatley FW. Observations of subchondral plate advancement during osteochondral repair: a histomorphometric and mechanical study in the rabbit femoral condyle. Osteoarthritis Cartilage 2003;11(11):810–820
82 Chen HM, Chevrier A, Hoemann CD, Sun J, Ouyang W, Buschmann MD. Characterization of subchondral bone repair for marrow-stimulated chondral defects and its relationship to articular cartilage resurfacing. Am J Sports Med 2011;39(8):1731–1740
83 Mainil-Varlet P, Van Damme B, Nesic D, Knutsen G, Kandel R, Roberts S. A new histology scoring system for the assessment of the quality of human cartilage repair: ICRS II. Am J Sports Med 2010;38(5):880–890
84 Saris DB, Vanlauwe J, Victor J, et al. Characterized chondrocyte implantation results in better structural repair when treating symptomatic cartilage defects of the knee in a randomized controlled trial versus microfracture. Am J Sports Med 2008;36(2):235–246
85 Vanlauwe J, Saris DBF, Victor J, Almqvist KF, Bellemans J, Luyten FP; TIG/ACT/01/2000&EXT Study Group. Five-year outcome of characterized chondrocyte implantation versus microfracture for symptomatic cartilage defects of the knee: early treatment matters. Am J Sports Med 2011;39(12):2566–2574
86 Brittberg M, Lindahl A, Nilsson A, Ohlsson C, Isaksson O, Peterson L. Treatment of deep cartilage defects in the knee with autologous chondrocyte transplantation. N Engl J Med 1994;331(14):889–895
87 Hoemann CD, Tran-Khan N, Méthot S, et al. Correlation of tissue histomorphometry with ICRS histology scores in biopsies obtained from a randomized controlled clinical trial comparing BST-CarGel™ versus microfracture. Paper presented at: International Cartilage Repair Society, 27 Sept, 2010; Barcelona, Spain
88 Méthot S, Hoemann CD, Rossomacha E, et al. ICRS Histology Scores of Biopsies from an Interim Analysis of a Randomized Controlled Clinical Trial Show Significant Improvement in Tissue Quality at 13 Months for BST-CarGel versus Microfracture. Paper presented at: International Cartilage Repair Society, 27 Sept, 2010; Barcelona, Spain
89 Changoor A, Nelea M, Méthot S, et al. Structural characteristics of the collagen network in human normal, degraded and repair articular cartilages observed in polarized light and scanning electron microscopies. Osteoarthritis Cartilage 2011;19(12):1458–1468
90 Roos EM, Engelhart L, Ranstam J, et al. ICRS Recommendation Document: Patient-Reported Outcome Instruments for Use in Patients with Articular Cartilage Defects. Cartilage 2011;2(2):122–136
91 Lascau-Coman V, Buschmann MD, Hoemann CD. Rapid EDTA Microwave Decalcification of Rabbit Osteochondral Samples Preserves Enzyme Activity and Antigen Epitopes. J Bone Miner Res 2008;23:S408–S408
92 Chevrier A, Rossomacha E, Buschmann MD, Hoemann CD. Optimization of histoprocessing methods to detect glycosaminoglycan, collagen type II, and collagen type I in decalcified rabbit osteochondral sections. J Histotechnol 2005;28(3):165–175